Original Article

Involvement of reactive oxygen species derived from mitochondria in neuronal injury elicited by methylmercury

Yasuhiro Ishihara,[1,*] Mayumi Tsuji,[2] Toshihiro Kawamoto[2] and Takeshi Yamazaki[1]

[1]Laboratory of Molecular Brain Science, Graduate School of Integrated Arts and Sciences, Hiroshima University, 1-7-1 Kagamiyama, Higashi-Hiroshima 739-8521, Japan
[2]Department of Environmental Health, University of Occupational and Environmental Health, 1-1 Iseigaoka, Yahata-nishi-ku, Kitakyushu, Fukuoka 807-8555, Japan

(Received 11 February, 2016; Accepted 4 June, 2016; Published online 7 October, 2016)

Methylmercury induces oxidative stress and subsequent neuronal injury. However, the mechanism by which methylmercury elicits reactive oxygen species (ROS) production remains under debate. In this study, we investigated the involvement of mitochondrial ROS in methylmercury-induced neuronal cell injury using human neuroblastoma SH-SY5Y-derived ρ^0 cells, which have a deletion of mitochondrial DNA and thus decreased respiratory activity. SH-SY5Y cells were cultured for 60 days in the presence of ethidium bromide to produce ρ^0 cells. Our ρ^0 cells showed decreases in the cytochrome *c* oxidase expression and activity as well as oxygen consumption compared with original SH-SY5Y cells. Methylmercury at a concentration of 1 μM induced cell death with oxidative stress in original SH-SY5Y cells, but not ρ^0 cells, indicating that ρ^0 cells are resistant to methylmercury-induced oxidative stress. ρ^0 cells also showed tolerance against hydrogen peroxide and superoxide anion, suggesting that ρ^0 cells are resistant to total ROS. These data indicate that mitochondrial ROS are clearly involved in oxidative stress and subsequent cell death induced by methylmercury. Considering that the dominant mechanism of ROS generation elicited by methylmercury is due to direct antioxidant enzyme inhibition, mitochondria might play a role in amplifying ROS in methylmercury-induced neurotoxicity.

***Key Words*:** **methylmercury, reactive oxygen species, mitochondria, neurotoxicity, ρ^0 cells**

Methylmercury is an organic heavy metal compound that is widely distributed in nature. Methylmercury is concentrated in aquatic animals through the food chain and becomes incorporated into human via seafood. Once methylmercury is taken up into the body, it is absorbed through the intestines into the blood and then reaches the brain by easily passing through the blood-brain barrier. Therefore, methylmercury shows strong neurotoxicity. Because methylmercury is re-absorbed in the intestine after being conjugated with reduced glutathione to excrete into bile, the half-life of methylmercury (approximately 70 days) is longer than that of other metal compounds. The cardinal symptoms of methylmercury intoxication are cerebellar ataxia, concentric contraction of visual field, auditory disorder and dysarthria, which are considered to be derived from degeneration in central nervous system.[1,2] In fact, high concentrations of methylmercury were detected in the brain of Minamata disease patients,[3] and several pathological findings such as cell shedding at the granular layer, precentral cortex and auditory cortices and abnormal proliferation of astrocytes in the calcarine cortex and cerebellar granular layer were observed.[2,4]

Oxidative stress is involved in neuronal injury induced by methylmercury. Oxidative cellular injury was elicited in human primary neurons and neuronal cell lines treated with methylmercury.[5,6] Methylmercury-treated mice showed high contents of lipid peroxides in the brain.[7] The mechanism by which methylmercury induces reactive oxygen species (ROS) generation in neurons is primarily considered to be due to the inhibition of antioxidant enzymes by methylmercury. Methylmercury is reported to directly bind to the selenocysteine residue in glutathione peroxidase (GPx) to increase the intracellular levels of hydrogen peroxide.[8] Methylmercury also inhibits glutathione reductase to suppress the re-generation of reduced glutathione,[9] leading to the potentiation of GPx inhibition. In addition, methylmercury reportedly inhibits thioredoxin and thioredoxin reductase to attenuate ROS elimination.[10,11] However, antioxidant enzymes can complement the ROS-eliminating capacity of another enzyme; that is, catalase efficiently scavenges hydrogen peroxide even under GPx inhabitable conditions.[12] Therefore, decreases in an antioxidant enzyme activity might not explain oxidative neuronal injury induced by methylmercury.

Metal ions such as iron and copper catalyze the Haber-Weiss reaction (Fenton reaction) to non-stoichiometrically produce high concentrations of reactive species and hydroxyl radicals.[13] Quinone compounds generate substantial amounts of superoxide anions via the redox cycle, which is repeated with quinone reduction by several reductases and quinone autooxidation by oxygen, leading to cellular injury.[14] However, methylmercury does not have catalytic activity in the Haber-Weiss reaction and furthermore cannot elicit the redox cycle. ROS-induced ROS release was recently proposed as a mitochondrial mechanism to amplify ROS.[15] Upon ROS-induced ROS release, mitochondria reportedly produce large amounts of ROS via the mitochondrial permeability transition and/or inner membrane anion channel just after low levels of ROS stimulate mitochondria, followed by cellular damage. ROS-induced ROS release is mainly observed in mitochondria-rich tissue such as the myocardium.[16]

As described above, ROS generation induced by methylmercury is mainly due to enzyme inhibition, and few reports have demonstrated that methylmercury directly acts on mitochondria. However, considering that mitochondria are abundant in the brain because of the requirement for substantial energy consumption, mitochondria could generate massive levels of ROS when exposed to methylmercury. In this study, we investigated the role of mitochondria in methylmercury-induced ROS generation and neuronal cell death using human neuroblastoma SH-SH5H-derived ρ^0 cells, which are depleted of mitochondrial DNA and thus have quite low respiratory activity.

*To whom correspondence should be addressed.
E-mail: ishiyasu@hiroshima-u.ac.jp

doi: 10.3164/jcbn.16-19

Materials and Methods

Materials. Methylmercury (II) chloride was purchased from Kanto Chemical (Tokyo, Japan). Cytochrome *c* and xanthine oxidase were obtained from Sigma-Aldrich (St. Louis, MO). Hydrogen peroxide was purchased from Wako Pure Chem. Ind., Ltd. (Osaka, Japan). H_2DCF-DA and Amplex Red were purchased from Molecular Probes (Eugene, OR). Ethidium bromide was purchased from Nacalai Tesque (Kyoto, Japan). Xanthine was obtained from Merck Millipore (Billerica, MA). All other chemicals were obtained from Wako Pure Chem. Ind. or Sigma-Aldrich and were of reagent grade.

Cell culture. Human neuroblastoma SH-SY5Y cells (CRL-2266, American Type Culture Collection, Manassas, VA) were placed into culture dishes and cultured in DMEM supplemented with 10% FBS as previously described.[17] The media were replaced every 3–4 days. Cells were sub-cultured when they reached 80–90% confluence.

Preparation of ρ^0 cells. Differentiation of SH-SY5Y cells was induced according to a previous report.[18] Briefly, SH-SY5Y cells were cultured in the presence of 100 μg/ml pyruvate, 50 μg/ml uridine and 0.5 or 2 μg/ml ethidium bromide for 60 days. The medium was changed every 2 day and the cells were replated approximately once per week.

Measurement of mitochondrial DNA content. To verify mitochondrial DNA depletion in ρ^0 cells, total cellular DNA was extracted by NucleoSpin Tissue kit (TaKaRa Bio, Kusatsu, Japan), and subjected to PCR amplification using mitochondrial DNA specific primers listed in Table 1. As a control, we measured glyceraldehyde-3-phosphate dehydrogenase DNA, which is coded in nuclear DNA. The band intensity was quantified using the Image J software program (NIH, Bethesda, MD).

Preparation of the mitochondrial fraction. Cells were collected and homogenized in a homogenization buffer containing 10 mM Tris-HCl, pH 7.4, 1 mM EDTA, 0.32 M Sucrose, 2.5 mg/ml BSA and 0.3 mM PMSF using the Dounce tissue grinder. The homogenate was centrifuged at 500 × *g* for 5 min at 4°C, and then the supernatant was centrifuged at 15,000 × *g* for 15 min at 4°C. The resulting pellet was resuspended in the homogenization buffer without BSA and PMSF and subsequently used as the mitochondrial fraction.

Immunoblotting. Cells were lysed with RIPA buffer (25 mM Tris-HCl, pH 7.6, 150 mM NaCl, 1% NP-40, 1% sodium deoxycholate, and 0.1% SDS), and then loaded and separated using SDS-PAGE with a 15% polyacrylamide gel and transferred onto a polyvinylidene difluoride (PVDF) membrane. The blocked membranes were incubated with anti-cytochrome *c* oxidase subunit IV antibody (1:2,000, Molecular Probes) or anti-α-tubulin antibody (1:2,000, Sigma-Aldrich). The membranes were incubated with peroxide-conjugated secondary antibodies (Thermo Fisher Scientific, Waltham, MA) and then visualized using peroxide substrates (SuperSignal West Femto, Thermo Fisher Scientific).

Measurement of cytochrome *c* oxidase activity. Isolated mitochondria were mixed with cytochrome *c* [final 0.7 % (w/v)] in 10 mM potassium phosphate buffer, pH 7.0. Then, decreases in absorbance at 550 nm were measured for 5 min. The activity of cytochrome *c* oxidase was calculated using the absorption coefficient of reduced cytochrome *c* (19.1 $mM^{-1}cm^{-1}$) and expressed as nmol/min/mg protein.[19]

Measurement of oxygen consumption. Oxygen concentration in the medium was estimated using the MitoXpress Xtra Oxygen Consumption Assay (Luxcel Biosciences Ltd., Cork, Ireland) according to the manufacturer's instructions. The oxygen-sensing fluorophore, MitoXpress Xtra, is quenched by oxygen through molecular collision, and thus the amount of fluorescence signal is inversely proportional to the amount of oxygen concentration.[20]

Determination of intracellular ATP levels. The intracellular ATP content was measured using a CellTiter-Glo Luminescent Cell Viability Assay Kit (Promega, Madison, WI) as described by our previous report.[21] Known concentrations of ATP were used as a standard.

Measurement of cell viability. Cellular viability was estimated as the percentage of lactate dehydrogenase activity in the medium and measured as described in our previous report.[22] The percentage of lactate dehydrogenase activity in the medium was calculated by dividing the activity in the medium by the total (medium + lysate) activity and expressed as the percent lactate dehydrogenase release.

Measurement of ROS levels. ROS levels inside cells were determined using H_2DCF-DA as a fluorescent probe, as described in our previous report with slight modification.[23] Cells were incubated with 10 μM H_2DCF-DA for 10 min under the culture conditions. Cells were then washed twice with ice-cold phosphate-buffered saline (PBS) and then fluorescence was measured by a FlexStation reader (Molecular Devices, Sunnyvale, CA) at an excitation wavelength of 504 nm and emission wavelength of 525 nm.

The hydrogen peroxide concentration in the culture medium was measured using Amplex Red (10-acetyl-3,7-dihydroxyphenoxazine), as previously reported.[24] Briefly, culture medium was mixed with Amplex Red in the presence of horseradish peroxidase. After a 30-min incubation in the dark, the fluorescence was measured by a FlexStation reader (Molecular Devices) at an excitation wavelength of 544 nm and emission wavelength of 590 nm. Known concentrations of hydrogen peroxide were used as a standard.

Observation of nuclear morphology. To assess chromatin condensation, DNA binding fluorochrome Hoechst 33342 was

Table 1. Primer sequences used in the detection of mitochondrial DNA

Target	Forward primer	Reverse primer	Product length (bp)
Mitochondrial DNA 1 (MtDNA1)	CCTAGGGATAACAGCGCAAT	TAGAAGAGCGATGGTGAGAG	630
Mitochondrial DNA 2 (MtDNA2)	AACATACCCATGGCCAACCT	GGCAGGAGTAATCAGAGGTG	532
GAPDH	ACCACAGTCCATGCCATCAC	CAGGAAATGAGCTTGACAAA	412

Table 2. Primer sequences used in real-time PCR

Gene	Forward primer	Reverse primer	Product length (bp)
SOD1*	CTGTACCAGTGCAGGTCCTC	CCAAGTCTCCAACATGCCTCT	86
Catalase	CTCCGGAACAACAGCCTTCT	ATAGAATGCCCGCACCTGAG	110
GPx1	TATCGAGAATGTGGCGTCCC	TCTTGGCGTTCTCCTGATGC	143
GCS*	CGGAGGAACAATGTCCGAGT	CCAGGACAGCCTAATCTGGG	132
β-actin	ACAGAGCCTCGCCTTTGC	ATCATCCATGGTGAGCTGGC	64

*Superoxide dismutase 1, SOD1; γ-glutamylcysteine synthetase, GCS.

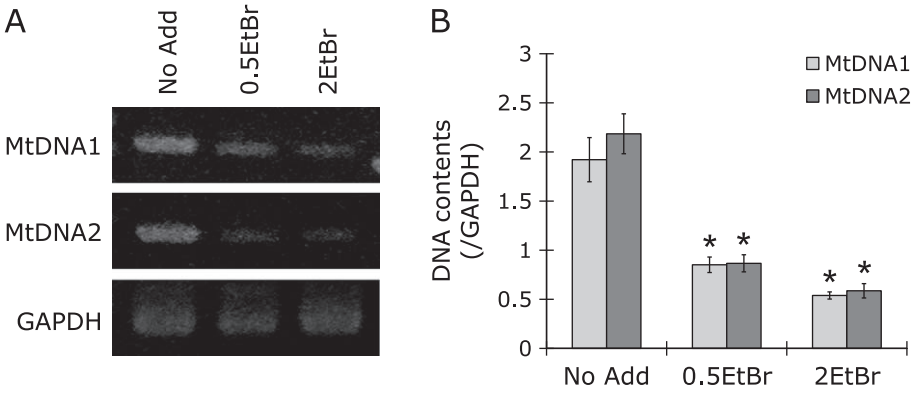

Fig. 1. Decreases in mitochondrial DNA contents in ethidium bromide-treated SH-SY5Y cells. SH-SY5Y cells were cultured for 60 days with 0.5 μg/ml (0.5EtBr) or 2 μg/ml ethidium bromide (2EtBr), respectively. SH-SY5Y cells cultured in the absence of ethidium bromide for 60 days were used as control (No Add). Total cellular DNA was extracted and then the content of mitochondrial DNA (MtDNA1 and MtDNA2) was measured by PCR. Representative images were shown as panel. (A) GAPDH, which is coded in nuclear DNA, was used as control. (B) The band density was measured using the Image J software program. The values are expressed as the means ± SEM of 4 separate experiments. *p<0.01 vs No Add group.

used. Hoechst 33342 was added to each well to a final concentration of 5 μg/ml and cells were incubated for 5 min at room temperature. The fluorescence was observed by a BZ-9000 inverted fluorescent microscope (Keyence, Osaka, Japan) at 360 ± 40 nm excitation, with a 460 ± 50 nm band-pass filter.

Measurement of caspase-3/7 activity. Caspase-3/7 activity was determined by a Caspase-Glo 3/7 Assay (Promega, Madison, WI), according to manufacturers' instruction. The luminescence was measured by a FlexStation reader (Molecular Devices).

Total RNA extraction and real-time PCR. Determination of mRNA levels was performed as previously described.[25] Briefly, total RNA was extracted from microglia using a High Pure RNA Isolation Kit (Roche Diagnostics K.K., Tokyo, Japan). Single-stranded cDNA was synthesized from 0.5 μg of total RNA following the ReverTra Ace protocol (Toyobo, Osaka, Japan) with a random primer (9-mer; Takara Bio, Shiga, Japan). Real-time PCR was performed with 50 cycles amplification using a LightCycler instrument (Roche Diagnostics) in a total reaction mixture volume of 10 μl containing 5 μl of Sybr Green Real-time PCR master mix (Toyobo), 1 μl cDNA solution and 5 pmol of each of the primers. The primer sequences used are listed in Table 2. The levels of mRNA were normalized to the β-actin mRNA level, and the values of ρ^0 cells were divided by those of original SH-SY5Y cells to give relative mRNA levels.

Statistical analyses. All data are expressed as the mean ± SEM. The statistical analyses were performed using one-way analysis of variance (ANOVA), followed by Student's t test or Dunnett's test. Multiple comparisons were made using Holm's or Bonferroni correction methods. Probability (p) values of <0.05 were considered to be statistically significant.

Results

Preparation and characterization of ρ^0 cells. Mitochondrial DNA of SH-SY5Y cells is reported to be depleted when cells are cultured in the presence of ethidium bromide.[18] Therefore, SH-SY5Y cells were cultured in the presence of 0.5 μg/ml or 2 μg/ml ethidium bromide for 60 days to prepare ρ^0 cells, which are represented as 0.5EtBr-ρ^0 cells and 2EtBr-ρ^0 cells, respectively, in this study. To verify the mitochondrial DNA depletion, total cellular DNA was extracted and subjected to PCR using mitochondrial DNA specific primers. 0.5EtBr-ρ^0 cells and 2EtBr-ρ^0 cells contained equivalent amounts of GAPDH (Fig. 1A), indicating that levels of nuclear DNA is similar among three types of cells. However, 0.5EtBr-ρ^0 cells and 2EtBr-ρ^0 cells contained less mitochondrial DNA than untreated cells (Fig. 1A and B). ρ^0 cells have been reported to show decreases in cytochrome c oxidase activity in the mitochondrial respiratory chain.[18] Therefore, we next characterized our ρ^0 cells, focusing on cytochrome c oxidase. The protein levels of cytochrome c oxidase subunit IV

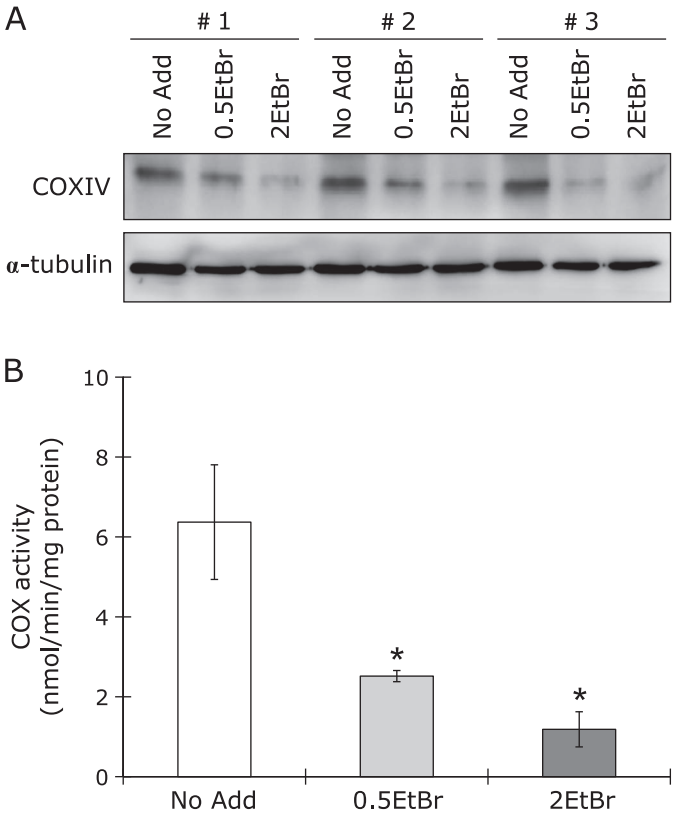

Fig. 2. Decreases in the expression and activity of cytochrome c oxidase in ethidium bromide-treated SH-SY5Y cells. SH-SY5Y cells were cultured for 60 days in the absence (No Add) or presence of 0.5 μg/ml (0.5EtBr) or 2 μg/ml ethidium bromide (2EtBr), respectively. (A) Protein levels of cytochrome c oxidase subunit IV (COX IV) were evaluated by immunoblotting. Images of 3 independent experiments are shown as the number 1 to 3. (B) The activity of cytochrome c oxidase (COX) was measured using cytochrome c as a substrate. The values are expressed as the means ± SEM of 4–5 separate experiments. *p<0.01 vs No Add group.

doi: 10.3164/jcbn.16-19

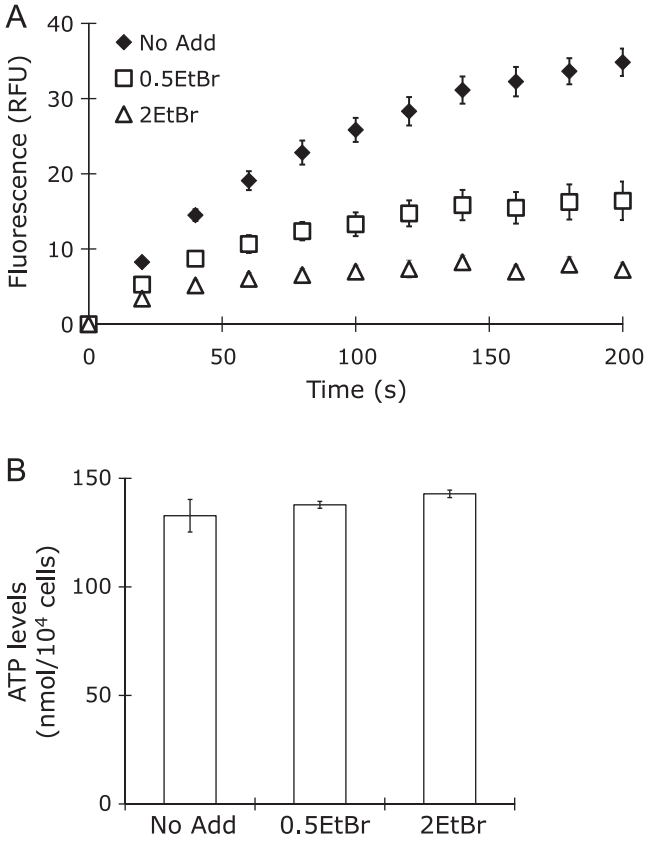

Fig. 3. Decreases in oxygen consumption in SH-SY5Y cells treated with ethidium bromide. SH-SY5Y cells were cultured for 60 days in the absence (No Add) or presence of 0.5 μg/ml (0.5EtBr) or 2 μg/ml ethidium bromide (2EtBr), respectively. (A) Cellular oxygen consumption was measured using an oxygen sensitive dye, MitoXpress. The values are expressed as the means ± SEM of 6 separate experiments. (B) Intracellular ATP levels were evaluated by a luminescent assay. The values are expressed as the means ± SEM of 8 separate experiments.

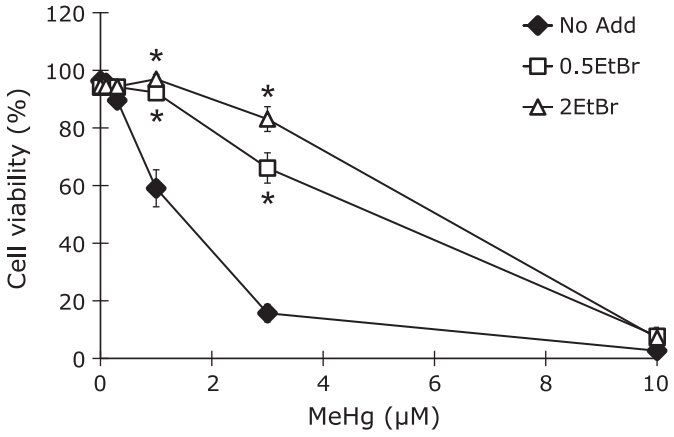

Fig. 4. Suppression of methylmercury-elicited toxicity in ρ^0 cells. SH-SY5Y cells were cultured for 60 days in the absence (No Add) or presence of 0.5 μg/ml (0.5EtBr) or 2 μg/ml ethidium bromide (2EtBr), respectively. Cells were treated with 0.1, 0.3, 1, 3 or 10 μM methylmercury (MeHg) for 24 h, and then cell viability was assessed using the lactate dehydrogenase leakage assay. The values are expressed as the means ± SEM of 4 separate experiments. *p<0.01 vs No Add group.

decreased following treatment with ethidium bromide in a concentration-dependent manner (Fig. 2A). In addition, the cytochrome *c* oxidase activity was also reduced by the addition of ethidium bromide (Fig. 2B), suggesting a low mitochondrial respiration activity. When we measured cellular oxygen consumption using an oxygen-sensing dye, MitoXpress, which indicates a high phosphorescence under hypoxic condition, SH-SY5Y cells showed a time-dependent increment in phosphorescence (Fig. 3A). However, phosphorescence derived from 0.5EtBr-ρ^0 cells and 2EtBr-ρ^0 cells was lower than that of original SH-SY5Y cells (Fig. 3A). The intracellular ATP levels were nearly the same among SH-SY5Y cells, 0.5EtBr-ρ^0 cells and 2EtBr-ρ^0 cells (Fig. 3B). These results indicate that the mitochondrial respiratory function is largely lost in 0.5EtBr-ρ^0 cells and 2EtBr-ρ^0 cells.

Tolerance to methylmercury-induced oxidative stress and cell death in ρ^0 cells. We next examined the tolerance of ρ^0 cells to methylmercury-induced oxidative stress and toxicity. When SH-SY5Y cells were treated with methylmercury for 24 h, approximately 40% of cells died following treatment at 1 μM methylmercury and almost all cells died following treatment at

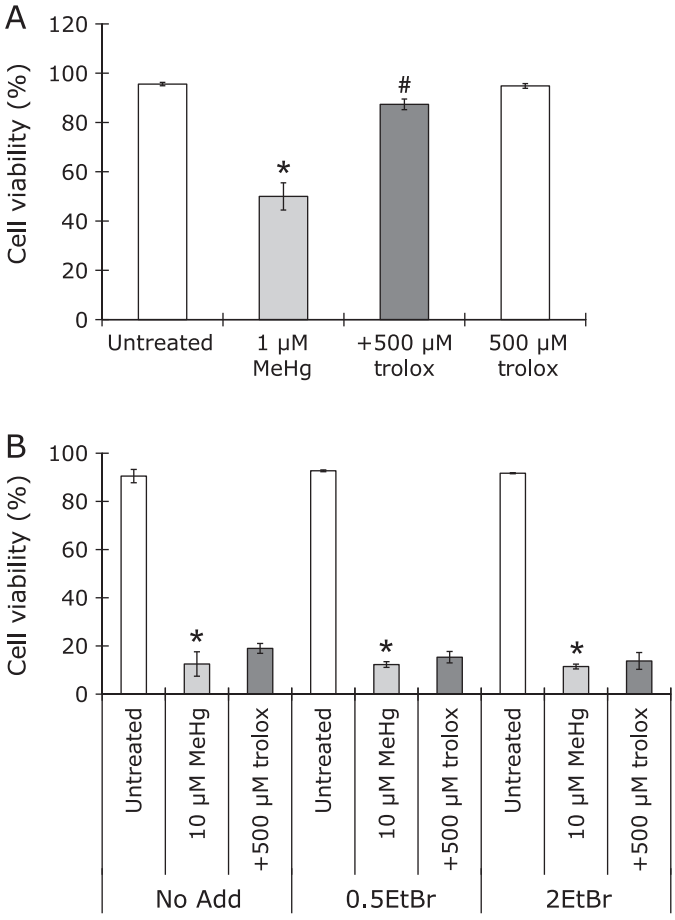

Fig. 5. Effects of an antioxidant, trolox, on methylmercury-induced cell death. SH-SY5Y cells were cultured for 60 days in the absence (No Add) or presence of 0.5 μg/ml (0.5EtBr) or 2 μg/ml ethidium bromide (2EtBr), respectively. (A) Cells were pretreated with 500 μM trolox for 20 min, followed by treatment with 1 μM methylmercury (MeHg) for 24 h. Cell viability was measured using the lactate dehydrogenase leakage assay. The values are expressed as the means ± SEM of 4 separate experiments. *p<0.01 vs untreated group. #p<0.01 vs MeHg-treated group. (B) Cells were pretreated with 500 μM trolox for 20 min and subsequently treated with 10 μM MeHg for 24 h. Cell viability was evaluated using the lactate dehydrogenase leakage assay. *p<0.01 vs untreated group.

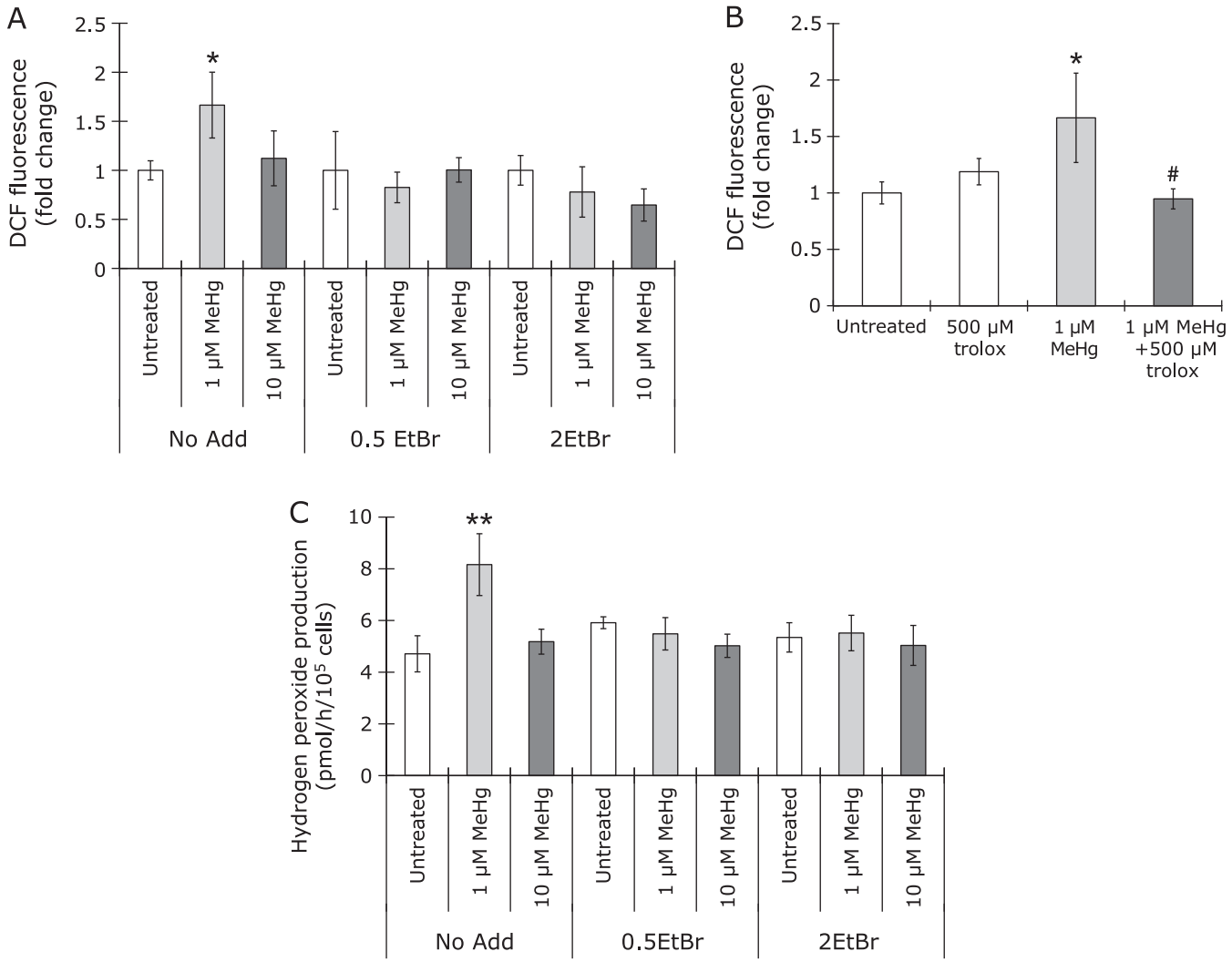

Fig. 6. Increases in ROS levels by methylmercury in SH-SY5Y cells, but not ρ^0 cells. SH-SY5Y cells were cultured for 60 days in the absence (No Add) or presence of 0.5 μg/ml (0.5EtBr) or 2 μg/ml ethidium bromide (2EtBr), respectively. (A, B) Cells were pretreated with 500 μM trolox for 20 min, followed by treatment with 1 or 10 μM methylmercury (MeHg) for 30 min. Intracellular ROS levels were measured using a fluorescent ROS probe, H_2DCF-DA. The values are expressed as the means ± SEM of 6 separate experiments. *p<0.05 vs untreated group. #p<0.05 vs 1 μM MeHg-treated group. (C) Cells were pretreated with 500 μM trolox for 20 min, followed by treatment with 1 or 10 μM MeHg for 3 h. Hydrogen peroxide content in the culture media was measured using a fluorescent dye, Amplex Red. The values are expressed as the means ± SEM of 4 separate experiments. **p<0.01 vs untreated group.

10 μM methylmercury (Fig. 4). Notably, 1 μM methylmercury did not elicit cell death in 0.5EtBr-ρ^0 cells and 2EtBr-ρ^0 cells (Fig. 4). Methylmercury at the concentration of 10 μM caused cell death of 0.5EtBr-ρ^0 cells and 2EtBr-ρ^0 cells, as observed in original SH-SY5Y cells (Fig. 4). Therefore, these data indicate that ρ^0 cells carry a higher tolerance to lower concentrations of methylmercury compared with original SH-SY5Y cells. An antioxidant, trolox, clearly suppressed cell death induced by methylmercury at a concentration of 1 μM (Fig. 5A), although trolox did not affect cellular injury elicited by treatment with 10 μM methylmercury (Fig. 5B). Challenge with H_2DCF-DA, a fluorescent probe for ROS, showed that the intracellular ROS levels increased by treatment with 1 μM methylmercury in SH-SY5Y cells and pretreatment with trolox clearly attenuated the increment in ROS (Fig. 6A and B), while 1 μM methylmercury had no effect on the intracellular ROS levels in 0.5EtBr-ρ^0 cells and 2EtBr-ρ^0 cells (Fig. 6A). In addition, the hydrogen peroxide levels in culture medium were elevated by treatment with 1 μM methylmercury in SH-SY5Y cells, but not in 0.5EtBr-ρ^0 cells or 2EtBr-ρ^0 cells (Fig. 6C). Methylmercury at the concentration of 10 μM did not cause any increment in hydrogen peroxide among SH-SY5Y cells, 0.5EtBr-ρ^0 cells and 2EtBr-ρ^0 cells (Fig. 6C). These results indicate that methylmercury at the concentration of 1 μM induces oxidative stress and subsequent cell death in SH-SY5Y cells, while methylmercury at the concentration of 10 μM cause cell death in an oxidative stress-independent manner in 0.5EtBr-ρ^0 cells and 2EtBr-ρ^0 cells.

Characterization of cell death induced in ρ^0 cells. Methylmercury is suggested to induce apoptotic cell death in neuronal cells.[8] Thus, we next characterized types of cell death induced by methylmercury from nuclear morphology and caspase activity. Nuclear staining by Hoechst 33342 showed the chromatin condensation induced by 1 μM methylmercury in SH-SY5Y cells: 12.9 ± 1.6% cells exhibited condensed nuclei, while methylmercury at the concentration of 10 μM did not affect nuclear morphology during cell death among SH-SY5Y cells, 0.5EtBr-ρ^0 cells and 2EtBr-ρ^0 cells (Fig. 7A). Caspase-3/7 activity increased in SH-SY5Y cells 24 h after treatment with 1 μM methylmercury

doi: 10.3164/jcbn.16-19

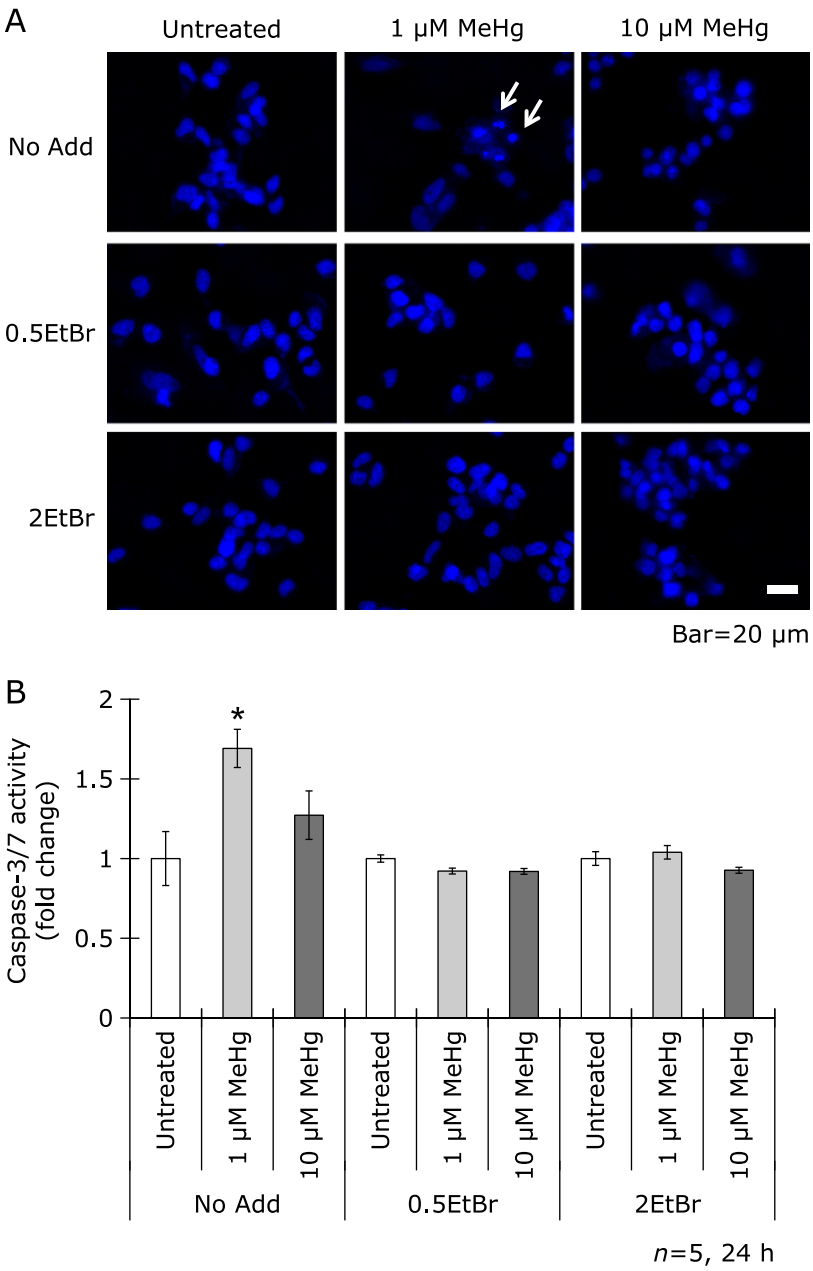

Fig. 7. Characterization of cell death induced by methylmercury. SH-SY5Y cells were cultured for 60 days in the absence (No Add) or presence of 0.5 μg/ml (0.5EtBr) or 2 μg/ml ethidium bromide (2EtBr), respectively. Cells were treated with 1 or 10 μM methylmercury (MeHg) for 24 h. (A) Chromatin condensation was assessed by Hoechst 33342 staining. Allows show condensed nuclei. (B) Cells were lysed and then caspase-3/7 activity was measured. The values are expressed as the means ± SEM of 4 separate experiments. *p<0.01 vs untreated group.

(Fig. 7B). However, when SH-SY5Y cells, 0.5EtBr-ρ^0 cells and 2EtBr-ρ^0 cells were administered with 10 μM methylmercury for 24 h, cells did not show any increment of caspase-3/7 activity (Fig. 7B). These results suggest that methylmercury at the concentration of 1 μM induces apoptotic cell death at least in part in SH-SY5Y cells, whereas 10 μM methylmercury elicits necrotic cell death in not only SH-SY5Y cells but also 0.5EtBr-ρ^0 cells and 2EtBr-ρ^0 cells.

Increment in oxidative stress tolerance of ρ^0 cells. Next, mechanism of methylmercury tolerance of ρ^0 cells was investigated. When we examined the mRNA expression of antioxidant enzymes in 0.5EtBr-ρ^0 cells and 2EtBr-ρ^0 cells, the mRNA levels of superoxide dismutase 1, catalase and γ-glutamylcysteine synthetase were significantly reduced compared with that in SH-SY5Y cells (Fig. 8). There was no change in GPx1 mRNA contents among SH-SY5Y cells, 0.5EtBr-ρ^0 cells and 2EtBr-ρ^0 cells (Fig. 8). Therefore, the high tolerance of 0.5EtBr-ρ^0 cells and 2EtBr-ρ^0 cells against oxidative injury accompanied with 1 μM methylmercury treatment could not be due to the modification of antioxidant enzyme expressions. Treatment with hydrogen peroxide or xanthine/xanthine oxidase, which generates superoxide anion by an enzymatic reaction, induced cell death in SH-SY5Y cells in a concentration-dependent manner (Fig. 9A and B). Interestingly, 0.5EtBr-ρ^0 cells and 2EtBr-ρ^0 cells showed higher resistances than SH-SY5Y cells to hydrogen peroxide or xanthine/xanthine oxidase (Fig. 9A and B), indicating that ρ^0 cells are

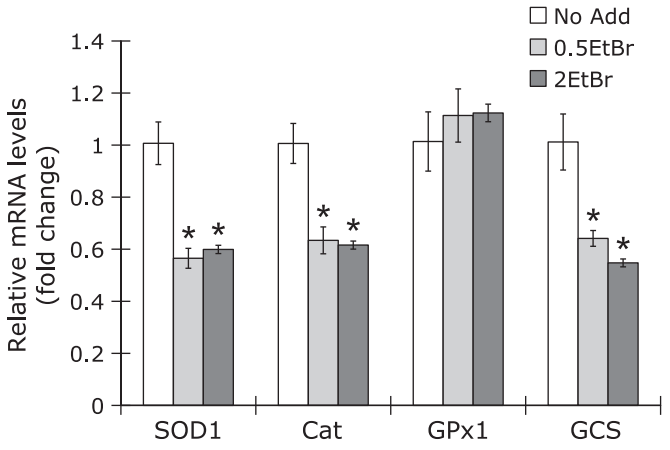

Fig. 8. Effects of ethidium bromide on the mRNA expression of antioxidant enzymes. SH-SY5Y cells were cultured for 60 days in the absence (No Add) or presence of 0.5 μg/ml (0.5EtBr) or 2 μg/ml ethidium bromide (2EtBr), respectively. The mRNA expression of antioxidant enzymes (Superoxide dismutase 1, SOD1; catalase; GPx1; γ-glutamylcysteine synthetase, GCS) was evaluated by real-time PCR. The mRNA levels are represented as the fold change from those in SH-SY5Y cells cultured without ethidium bromide. The values are expressed as the means ± SEM of 3 separate experiments. *p<0.01 vs No Add group.

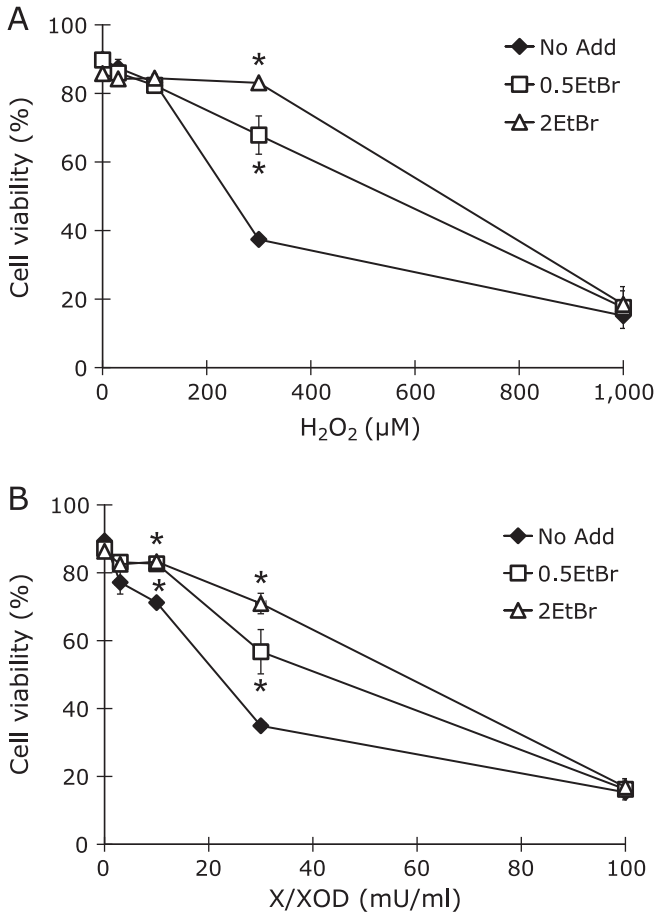

Fig. 9. Suppression of ROS-induced cell death in ρ^0 cells. SH-SY5Y cells were cultured for 60 days in the absence (No Add) or presence of 0.5 μg/ml (0.5EtBr) or 2 μg/ml ethidium bromide (2EtBr), respectively. The cells were then treated with oxidants: 30, 100, 300 or 1,000 μM hydrogen peroxide (H_2O_2) or 100 μM xanthine plus 3, 10, 30 or 100 mU/ml xanthine oxidase (X/XOD) for 24 h, and cell viability was assessed using the lactate dehydrogenase leakage assay. The values are expressed as the means ± SEM of 4 separate experiments. *p<0.01 vs No Add group.

resistant to ROS themselves as well as methylmercury-induced oxidative stress.

Lead and trimethyltin other than methylmercury are reported to induce oxidative stress and neuronal injury;[26,27] thus, we evaluated the toxicity of lead diacetate and trimethyltin in ρ^0 cells. Treatment with lead diacetate and trimethyltin elicited cell death in a dose-dependent manner in original SH-SY5Y cells (Fig. 10). Of note, cellular injury induced by lead diacetate and trimethyltin were significantly attenuated in 0.5EtBr-ρ^0 cells (Fig. 10). Therefore, mitochondria are considered to be involved in neuronal injury induced by metal compounds which cause oxidative stress.

Discussion

When several cell lines are cultured with relatively low concentrations of ethidium bromide for over 30 days, mitochondrial DNA is selectively deleted.[18,28] This type of cell is referred to as ρ^0 cells. Because a part of the respiratory complexes are encoded in mitochondrial DNA, ρ^0 cells show no or less activity of respiratory chain. ρ^0 cells have been used in studies to analyze the mitochondrial function, such as mitochondria-dependent apoptosis.[29] In this study, we produced ρ^0 cells derived from a human neuroblastoma cell line, SH-SY5Y, as previously described.[18] Miller *et al.*[18] reported that SH-SY5Y cells were cultured in the presence of 5 μg/ml ethidium bromide. However, treatment with ethidium bromide at this concentration largely decreased cell proliferation (data not shown). Thus, we cultured cells with 0.5 or 2 μg/ml ethidium bromide. Our ρ^0 cells showed large decreases in mitochondrial functions since the expression and activity of cytochrome *c* oxidase, as well as oxygen consumption were clearly reduced. Therefore, we examined the involvement of mitochondria in methylmercury-induced neurotoxicity using our ρ^0 cells.

Although ρ^0 cells produced in this study showed decreased respiratory chain activity, the intracellular ATP levels in ρ^0 cells were similar to those in original SH-SY5Y cells. The expression of lactate dehydrogenase was reportedly enhanced in ρ^0 cells.[30] Lactate dehydrogenase potentiates glycolysis by supplying NAD^+ to glyceraldehyde-3-phosphate dehydrogenase, which induces the enhancement of ATP synthesis during glycolysis. Therefore, ρ^0 cells could maintain ATP levels similar to that in original SH-SY5Y cells by enhancement of glycolysis activity.

Methylmercury at the concentration of 1 μM induced oxidative stress and subsequent cell death in SH-SY5Y cells because treatment with 1 μM methylmercury increased intracellular ROS levels and an antioxidant, trolox, clearly suppressed cell death. On the other hand, cell death induced by treatment with 10 μM methylmercury is not considered to be involved in oxidative stress as pretreatment with trolox failed to attenuate cell death induced by 10 μM methylmercury. Methylmercury is electrophilic and can highly react with thiols and selenocysteines. Cysteine residues in proteins have different pKa values that are dependent on the milieu, such as surrounding amino acids,[23] and thus have different reactivities with methylmercury. A low concentration of methylmercury specifically reacts with cysteine residues with low pKa values or selenocysteines, which are often included in active sites of antioxidant enzymes such as GPx or thioredoxin.[31,32] In this regard, a low concentration of methylmercury could elicit oxidative stress. It is considered that a high concentration of methylmercury reacts with any nucleophilic substance to cause toxicity. Indeed, inhibition of microtubule polymerization and suppression of *de novo* protein synthesis are reported to be toxic mechanisms of methylmercury.[33,34]

doi: 10.3164/jcbn.16-19

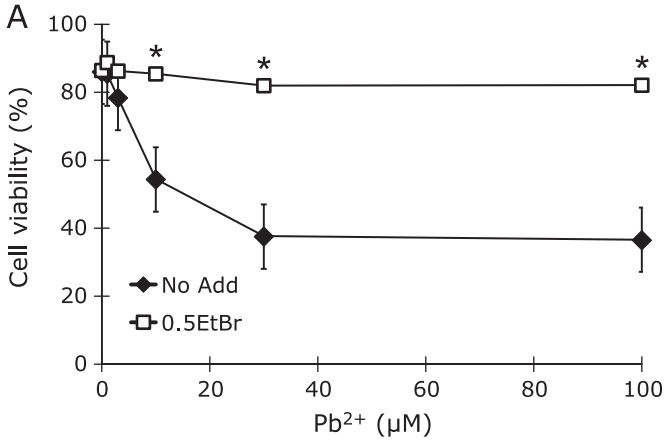

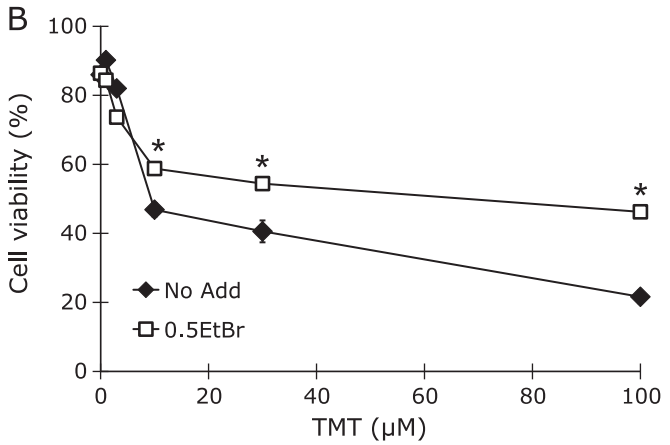

Fig. 10. Suppression of metal-induced toxicity in ρ^0 cells. SH-SY5Y cells were cultured for 60 days in the absence (No Add) or presence of 0.5 μg/ml ethidium bromide (0.5EtBr). Cells were treated with 1, 3, 10, 30 or 100 μM lead diacetate or trimethyltin (TMT) for 24 h. Cell viability was evaluated using the lactate dehydrogenase leakage assay. The values are expressed as the means ± SEM of 6 separate experiments. **p*<0.01 vs No Add group.

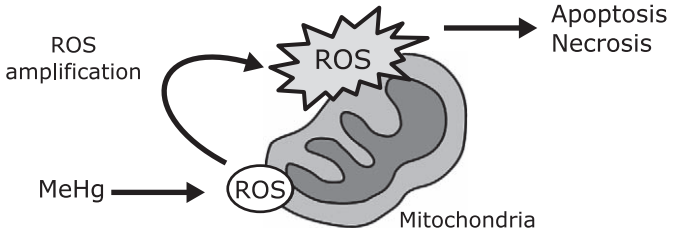

Fig. 11. Proposed model of the role of mitochondrial ROS in methylmercury-induced neuronal cell death. Mitochondria can amplify ROS by ROS-induced ROS release. Therefore, ROS generated by methylmercury (MeHg) mainly via the inhibition of antioxidant enzymes could act on mitochondria to amplify ROS, leading to oxidative cellular injury.

ρ^0 cells produced in this study showed resistance to methylmercury toxicity compared with original SH-SY5Y cells. As discussed above, the toxic mechanism accompanied by 1 μM methylmercury treatment is oxidative stress. The antioxidant enzyme expression in ρ^0 cells was relatively lower than that in SH-SY5Y cells. According to these results, cell death induced by 1 μM methylmercury in SH-SY5Y cells could be due to ROS derived from mitochondria. Although methylmercury is reported to act on mitochondrial respiratory complex II and III,[35] the primary mechanism of methylmercury-induced oxidative stress is due to the inhibition of antioxidant enzymes.[36] Increasing evidence shows that mitochondria can amplify ROS by ROS-induced ROS release.[15] Therefore, an explanation of the phenomena observed in this study is that methylmercury induces ROS production by direct inhibition of antioxidant enzymes and generated ROS subsequently act on mitochondria to amplify ROS by ROS-induced ROS release, leading to oxidative stress (Fig. 11). This hypothesis is supported by the finding that cell death induced by hydrogen peroxide or superoxide anion was suppressed in ρ^0 cells. Judging from Hoechst 33342 staining and caspase-3/7 activity, a part of cell death elicited by 1 μM methylmercury in SH-SY5Y cells is apoptotic. Therefore, ROS amplified in mitochondria are considered to be involved in both apoptotic and necrotic cell death. Antioxidant enzymes are known to complement their ROS scavenging activity. We have previously reported that inhibition of GPx or catalase alone did not cause cell death, whereas inhibition of both GPx and catalase induced oxidative stress and oxidative injury.[12,23] Therefore, specific inhibition of antioxidant enzymes induced by methylmercury might not be sufficient to elicit oxidative stress. Oxidative neuronal injury could occur with antioxidant enzyme inhibition and subsequent mitochondrial ROS amplification.

ρ^0 cells are reported to show resistance to mitochondrial apoptosis and proliferation induced by radiation.[29,37] Sulforaphane-induced ROS production is also known to be decreased in ρ^0 cells, however, this result is reasonable as sulforaphane has been shown to induce mitochondrial uncoupling to generate ROS.[38] In this study, cell death induced by lead and trimethyltin, in addition to methylmercury, was suppressed in ρ^0 cells compared with original SH-SY5Y cells. Lead is reported to increase the intracellular ROS levels by the inhibition of antioxidant enzymes.[26] We previously reported that organotin compounds elicited oxidative stress via glutathione *S*-transferase inhibition and subsequent suppression of peroxidation.[39] Therefore, mitochondrial ROS amplification might be involved in toxicity induced by lead or organotin compounds.

In conclusion, we investigated the involvement of mitochondrial ROS in methylmercury toxicity using ρ^0 cells derived from SH-SY5Y cells. ρ^0 cells were resistant to methylmercury-induced oxidative stress and cell death compared with original SH-SY5Y cells. The primary mechanism of ROS production by methylmercury is considered to be due to the inhibition of antioxidant enzymes, and mitochondria can amplify ROS by ROS-induced ROS release. Therefore, ROS amplification in mitochondria might be involved in methylmercury-induced oxidative neuronal injury.

Acknowledgments

This work was supported in part by grants (KAKENHI) from the Ministry of Education, Culture, Sports, Science, and Technology of Japan to Y.I. and T.Y. (26740024 and 22310041) and a grant from the Fujii Foundation to Y.I.

Conflict of Interest

No potential conflicts of interest were disclosed.

References

1 Eto K. Pathology of Minamata disease. *Toxicol Pathol* 1997; **25**: 614–623.
2 Shiraki H. Neuropathological aspects of organic mercury intoxication, including Minamata disease. In: Vinken PJ, Bruyn GW, eds. *Handbook of Clinical Neurology, Vol. 36*, Amsterdam: Elsevier, 1979; 83–145.
3 Eto K, Takizawa Y, Akagi H, *et al*. Differential diagnosis between organic and inorganic mercury poisoning in human cases--the pathologic point of view. *Toxicol Pathol* 1999; **27**: 664–671.
4 Takeuchi T, Morikawa N, Matsumoto H, Shiraishi Y. A pathological study of Minamata disease in Japan. *Acta Neruropathol* 1962; **2**: 40–57.
5 Sanfeliu C, Sebastià J, Ki SU. Methylmercury neurotoxicity in cultures of human neurons, astrocytes, neuroblastoma cells. *Neurotoxicology* 2001; **22**: 317–327.
6 Petroni D, Tsai J, Agrawal K, Mondal D, George W. Low-dose methylmercury-induced oxidative stress, cytotoxicity, and tau-hyperphosphorylation in human neuroblastoma (SH-SY5Y) cells. *Environ Toxicol* 2012; **27**: 549–555.
7 Carvalho MC, Franco JL, Ghizoni H, *et al*. Effects of 2,3-dimercapto-1-propanesulfonic acid (DMPS) on methylmercury-induced locomotor deficits and cerebellar toxicity in mice. *Toxicology* 2007; **239**: 195–203.
8 Franco JL, Posser T, Dunkley PR, *et al*. Methylmercury neurotoxicity is associated with inhibition of the antioxidant enzyme glutathione peroxidase. *Free Radic Biol Med* 2009; **47**: 449–457.
9 Stringari J, Nunes AK, Franco JL, *et al*. Prenatal methylmercury exposure hampers glutathione antioxidant system ontogenesis and causes long-lasting oxidative stress in the mouse brain. *Toxicol Appl Pharmacol* 2008; **227**: 147–154.
10 Carvalho CM, Chew EH, Hashemy SI, Lu J, Holmgren A. Inhibition of the human thioredoxin system. A molecular mechanism of mercury toxicity. *J Biol Chem* 2008; **283**: 11913–11923.
11 Wagner C, Sudati JH, Nogueira CW, Rocha JB. *In vivo* and *in vitro* inhibition of mice thioredoxin reductase by methylmercury. *Biometals* 2010; **23**: 1171–1177.
12 Ishihara Y, Shimamoto N. Critical role of exposure time to endogenous oxidative stress in hepatocyte apoptosis. *Redox Rep* 2007; **12**: 275–281.
13 Stohs SJ, Bagchi D. Oxidative mechanisms in the toxicity of metal ions. *Free Radic Biol Med* 1995; **18**: 321–336.
14 Ishihara Y, Shiba D, Shimamoto N. Enhancement of DMNQ-induced hepatocyte toxicity by cytochrome P450 inhibition. *Toxicol Appl Pharmacol* 2006; **214**: 109–117.
15 Zorov DB, Juhaszova M, Sollott SJ. Mitochondrial reactive oxygen species (ROS) and ROS-induced ROS release. *Physiol Rev* 2014; **94**: 909–950.
16 Biary N, Xie C, Kauffman J, Akar FG. Biophysical properties and functional consequences of reactive oxygen species (ROS)-induced ROS release in intact myocardium. *J Physiol* 2011; **589 (Pt 21)**: 5167–5179.
17 Ishihara Y, Itoh K, Ishida A, Yamazaki T. Selective estrogen-receptor modulators suppress microglial activation and neuronal cell death via an estrogen receptor-dependent pathway. *J Steroid Biochem Mol Biol* 2015; **145**: 85–93.
18 Miller SW, Trimmer PA, Parker WD Jr, Davis RE. Creation and characterization of mitochondrial DNA-depleted cell lines with "neuronal-like" properties. *J Neurochem* 1996; **67**: 1897–1907.
19 Wharton DC, Tzagoloff A. Cytochrome oxidase from beef heart mitochondria. *Methods Enzymol* 1967; **10**: 245–250.
20 Will Y, Hynes J, Ogurtsov VI, Papkovsky DB. Analysis of mitochondrial function using phosphorescent oxygen-sensitive probes. *Nat Protoc* 2006; **1**: 2563–2572.
21 Ishihara Y, Katayama K, Sakabe M, *et al*. Antioxidant properties of rare sugar D-allose: effects on mitochondrial reactive oxygen species production in Neuro2A cells. *J Biosci Bioeng* 2011; **112**: 638–642.
22 Ishihara Y, Takemoto T, Itoh K, Ishida A, Yamazaki T. Dual role of superoxide dismutase 2 induced in activated microglia: oxidative stress tolerance and convergence of inflammatory responses. *J Biol Chem* 2015; **290**: 22805–22817.
23 Ishihara Y, Shiba D, Shimamoto N. Primary hepatocyte apoptosis is unlikely to relate to caspase-3 activity under sustained endogenous oxidative stress. *Free Radic Res* 2005; **39**: 163–173.
24 Zhou M, Diwu Z, Panchuk-Voloshina N, Haugland RP. A stable nonfluorescent derivative of resorufin for the fluorometric determination of trace hydrogen peroxide: applications in detecting the activity of phagocyte NADPH oxidase and other oxidases. *Anal Biochem* 1997; **253**: 162–168.
25 Takemoto T, Ishihara Y, Ishida A, Yamazaki T. Neuroprotection elicited by nerve growth factor and brain-derived neurotrophic factor released from astrocytes in response to methylmercury. *Environ Toxicol Pharmacol* 2015; **40**: 199–205.
26 Patrick L. Lead toxicity part II: the role of free radical damage and the use of antioxidants in the pathology and treatment of lead toxicity. *Altern Med Rev* 2006; **11**: 114–127.
27 Yoneyama M, Nishiyama N, Shuto M, *et al*. *In vivo* depletion of endogenous glutathione facilitates trimethyltin-induced neuronal damage in the dentate gyrus of mice by enhancing oxidative stress. *Neurochem Int* 2008; **52**: 761–769.
28 King MP, Attardi G. Human cells lacking mtDNA: repopulation with exogenous mitochondria by complementation. *Science* 1989; **246**: 500–503.
29 Kim JY, Kim YH, Chang I, *et al*. Resistance of mitochondrial DNA-deficient cells to TRAIL: role of Bax in TRAIL-induced apoptosis. *Oncogene* 2002; **21**: 3139–3148.
30 Park KS, Nam KJ, Kim JW, *et al*. Depletion of mitochondrial DNA alters glucose metabolism in SK-Hep1 cells. *Am J Physiol Endocrinol Metab* 2001; **280**: E1007–E1014.
31 Sugiura Y, Tamai Y, Tanaka H. Selenium protection against mercury toxicity: high binding affinity of methylmercury by selenium-containing ligands in comparison with sulfur-containing ligands. *Bioinorg Chem* 1978; **9**: 167–180.
32 Forman-Kay JD, Clore GM, Gronenborn AM. Relationship between electrostatics and redox function in human thioredoxin: characterization of pH titration shifts using two-dimensional homo- and heteronuclear NMR. *Biochemistry* 1992; **31**: 3442–3452.
33 Miura K, Kobayashi Y, Toyoda H, Imura N. Methylmercury-induced microtubule depolymerization leads to inhibition of tubulin synthesis. *J Toxicol Sci* 1998; **23**: 379–388.
34 Cheung MK, Verity MA. Experimental methyl mercury neurotoxicity: locus of mercurial inhibition of brain protein synthesis *in vivo* and *in vitro*. *J Neurochem* 1985; **44**: 1799–1808.
35 Mori N, Yasutake A, Hirayama K. Comparative study of activities in reactive oxygen species production/defense system in mitochondria of rat brain and liver, and their susceptibility to methylmercury toxicity. *Arch Toxicol* 2007; **81**: 769–776.
36 Farina M, Aschner M, Rocha JB. Oxidative stress in MeHg-induced neurotoxicity. *Toxicol Appl Pharmacol* 2011; **256**: 405–417.
37 Cloos CR, Daniels DH, Kalen A, *et al*. Mitochondrial DNA depletion induces radioresistance by suppressing G_2 checkpoint activation in human pancreatic cancer cells. *Radiat Res* 2009; **171**: 581–587.
38 Xiao D, Powolny AA, Antosiewicz J, *et al*. Cellular responses to cancer chemopreventive agent D,L-sulforaphane in human prostate cancer cells are initiated by mitochondrial reactive oxygen species. *Pharm Res* 2009; **26**: 1729–1738.
39 Ishihara Y, Kawami T, Ishida A, Yamazaki T. Tributyltin induces oxidative stress and neuronal injury by inhibiting glutathione S-transferase in rat organotypic hippocampal slice cultures. *Neurochem Int* 2012; **60**: 782–790.

doi: 10.3164/jcbn.16-19